Title:
PGE-RANSAC: An Improved RANSAC-Based Robust Point Cloud Geometric Feature Extraction Algorithm

Authors:
Lei Lu, lulei@haut.edu.cn, Henan University of Technology
Ran Gao, gaorana2021@163.com, Henan University of Technology
Wei Pan, vpan@foxmail.com, OPT Machine Vision Tech Co., Ltd.
Wenming Tang, tangwenming@sziit.edu.cn, Shenzhen Institute of Information Technology

Keywords:
Three-Dimensional Image Processing, Object Detection, Random Sample Consensus, Geometric Figures, Point Cloud Processing

DOI: 10.14733/cadconfP.2024.312-317

Introduction:
Point cloud geometric feature extraction has garnered significant attention in machine vision and graphics and finds widespread application in fields such as reverse engineering and industrial inspection [1]. As the accuracy and resolution of three-dimensional (3D) scanning equipment, such as Lidar and 3D cameras, continue to improve, the volume of point cloud data is experiencing rapid growth, leading to increasingly complex data processing requirements and higher computing costs. [2]. Moreover, the presence of noise in acquired point cloud data and the complexity of geometric shapes pose challenges to accurate geometric feature retrieval. Therefore, there is a strong demand for efficient and accurate methods for extracting point cloud geometric features. [3].

RANSAC demonstrates superior performance and robustness in planar prediction; however, it suffers from the drawback of mistakenly identifying contiguous or adjacent planes as a single plane [4]. Additionally, existing boundary extraction algorithms exhibit low efficiency when processing large-scale point cloud data. [5]. To address these challenges, this paper introduces the PGE-RANSAC (Point Cloud Geometry Extraction-RANSAC) method for extracting point cloud geometric features. This method enhances the performance of the traditional RANSAC approach by incorporating the screening and judgment mechanism of principal component analysis (PCA). Furthermore, the efficiency of boundary extraction is enhanced by transforming the three-dimensional point cloud into a two-dimensional (2D) image. Ultimately, geometric features are extracted using a multilink clustering method. [6]. Experimental results demonstrate the effectiveness of the proposed method in extracting geometric shapes from point clouds.

Main Idea:
The proposed method comprises five sequential steps, as illustrated in Fig. 1. Initially, the original point cloud is acquired. Subsequently, employing PCA and RANSAC, the plane of the initial point cloud data is extracted, and plane segment optimization is achieved through consideration of the normal vector and Euclidean distance. To enhance processing speed, dimensionality reduction is implemented by transforming the 3D point cloud into a 2D image, enabling efficient boundary extraction. In the fourth step, boundary points are segmented based on predefined assumptions and a comparison framework. Finally, geometric features are derived by separately fitting the boundary point segmentations.

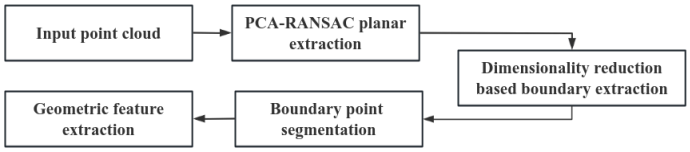

Fig. 1: Schematic diagram of the algorithm flow.

With the obtained point cloud data, the initial planar set is extracted based on RANSAC firstly. Assumes that P is an initial point cloud containing n points, and each point is represented as $p_i\ x_i,y_i,z_i$, $i \in [0,1,2,\ldots,n-1]$. In order to avoid incorrect fitting as much as possible, three points that are far away from each other are randomly selected as the sample point set S. The distance is determined by the average distance of points in the point cloud data. A plane is fitted based on S. The variance of the distance from all points to the plane is F:

$$F = \sum_{i=0}^{n-1} a_0 x_i + a_1 y_i + a_2 - z_i \ ^2 , \tag{2.1}$$

For each point in S minimizing F, we have $\frac{\partial F}{\partial a_0} = 0$、$\frac{\partial F}{\partial a_1} = 0$、$\frac{\partial F}{\partial a_2} = 0$. Then solve the system of equations to get the parameters a_0, a_1, a_2 , and the initial plane fitting is completed.

Then the outliers in the point cloud P is removed based on the initial fitting plane. Implement the above steps iteratively by N_{iterate} times and select the point set S including the largest number of points as the current plane prediction result. Remove the current plane point set from the initial point cloud P and select a new plane S to start a new round plane prediction until the number of the points is less than a threshold N_{minnum}. A series of point cloud sets $P_{\text{array}} = P_1, P_2, \ldots, P_{N_{\text{plane}}}$ can be obtained and N_{plane} is the number of extracted planes.

RANSAC demonstrates effective performance in scenarios where the point cloud exhibits significant noise. However, errors may arise when the noise level is comparable to that of the plane itself, such as in cases involving adjacent planes. This paper tackles the aforementioned challenge by introducing a PCA-based RANSAC (PCA-RANSAC) plane fitting method along with an optimization strategy.

At first, PCA plane fitting is applied to all the planes in point cloud sets P_{array}. Suppose that there are n_1 points in P_1. The centroid mx_1, my_1, mz_1 was used to centralize the point cloud and obtain the sample matrix $\mathbf{X_1}$.Calculate the corresponding covariance matrix $\mathbf{E_1}$:

$$\mathbf{E_1} = \frac{1}{n_1 - 1} \mathbf{X_1^T X_1} , \tag{2.2}$$

The eigenvalue decomposition of $\mathbf{E_1}$ is carried out to obtain its eigenvector and eigenvalue, select the eigenvector with the minimum eigenvalue as the plane normal vector $\mathbf{v_{normmall}}$, which is combined with the centroid to fit the plane.

Repeat the above process for each planar in P_{array} and N_{plane} planes are obtained. That planes are merged or removed by comparing the angles and distances between each other. The optimization

strategy is as follows: assume the normal vectors of plane 1 and plane 2 are $\mathbf{v}_{\mathbf{normmal1}}$ and $\mathbf{v}_{\mathbf{normmal2}}$ respectively, and their angles are defined as θ_{angle12}; the number of points for the two planes are n_{p1} and n_{p2}. When $n_{p1}+n_{p2} \geq N_{\text{minnum}}$ and $\theta_{\text{angle12}} < \theta_{\text{th}}$ (θ_{th} is the plane angle threshold determining whether the two planes need to be merged or not, which is set to 15° in this paper), calculate the distance from the point to plane 1 and the distance from the point to plane 2, respectively, if the proportion of the points whose distance is less than d_{th} is greater than 90%, the point sets of plane 1 and plane 2 are merged. In the other hand, if $n_{p1}+n_{p2} < N_{\text{minnum}}$, the point sets for planes 1 and 2 are removed. Where the d_{th} is the distance threshold that determines the merging of planes, depending on the actual accuracy required. The optimization strategy described above is applied iteratively to all planes until no further merging or removal can be performed.

To expedite boundary extraction, the dimensionality of the point cloud data is reduced by transforming the 3D data into a 2D image. Firstly, the orientation of the planar point cloud is adjusted to be parallel to the XOY plane based on Eq. (2.3). Secondly, Eq. (2.4) is utilized to transform the 3D point cloud data into a 2D image.

$$\begin{pmatrix} x' \\ y' \\ z' \\ 1 \end{pmatrix} = \mathbf{M}_{\mathbf{pose}} \begin{pmatrix} x \\ y \\ z \\ 1 \end{pmatrix}, \tag{2.3}$$

$$\begin{cases} u = \dfrac{y'}{f_x} + c_x \\ v = \dfrac{x'}{f_y} + c_y \end{cases}, \tag{2.4}$$

Where u and v are the row and column coordinates of the 2D image; f_x and f_y are focal lengths; c_x, c_y are offsets. The focal lengths and offsets are determined based on the camera parameters. To facilitate contour extraction, the intensity value of valid points on the object is set to 0, while points outside the object are set to 1. Subsequently, in order to extract the object boundary from the 2D image, a Gaussian function is applied to smooth the image. The smoothed image is then processed to obtain the gradient in the horizontal and vertical directions, as well as the gradient direction using the Sobel operator. Edge points can be identified based on the gradient information.

In order to extract the geometry from the boundary points, it is necessary to divide the boundary points into multiple segments. This paper proposes to use the hypothesis and comparison framework based on multilink clustering to segment the boundary points.

Firstly, the boundary points were preliminarily clustered based on the iterative RANSAC line fitting model and multiple straight lines were obtained by multiple RANSAC iterations. Secondly, apply dynamic fitting for each pair of closest clusters and employ f_{score} in Eq. (2.5) to decide whether to merge them or not.

$$f_{score}\ M_i = \frac{n_{in}}{n_{all}}, \tag{2.5}$$

Where M_i represents a cluster, n_{in} represents the number of points in the current cluster adaptation and fitting model, n_{all} represents the total number of points in the current cluster, and f_{score} is the

measurement result. Assuming that M_j represents another cluster closest to M_i, the Eq. (2.6) is used to merge them or not:

$$F\ M_i, M_j\ = \begin{cases} 1 & 2 * f_{score}\ M_i \cup M_j\ \geq f_{score}\ M_i\ + f_{score}\ M_j \\ 0 & 2 * f_{score}\ M_i \cup M_j\ < f_{score}\ M_i\ + f_{score}\ M_j \end{cases}, \tag{2.6}$$

Where $F\ M_i, M_j$ is the result of measuring whether to merge, if it equals to 1, it will be merged, and if it equals to 0, it will not be merged.

This paper conducts connectivity segmentation based on clustering to accomplish the segmentation of contour points. Finally, by fitting the straight lines in sequence, the vertices at the intersection of the straight lines are obtained. The corresponding points in the three-dimensional space are obtained by inversely transforming the point sets according to Eq. (2.4) and Eq. (2.3), thereby extracting the geometric figures in the point cloud.

Experiments and results:
The experimental objects and point clouds are shown in Fig. 2.

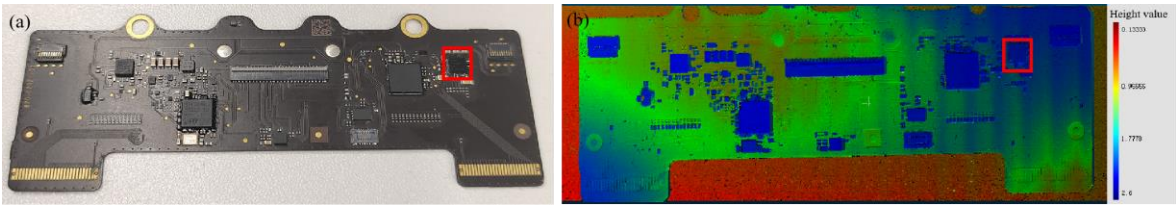

Fig. 2: Experimental object circuit board. (a) Physical drawing of the circuit board. (b) Schematic board point cloud.

To verify the effectiveness of the algorithm, the traditional RANSAC method and region growth algorithm is employed to process the same data for comparison [7]. The chip on the right side in Fig. 2 is selected and the comparison results are shown in Fig. 3.

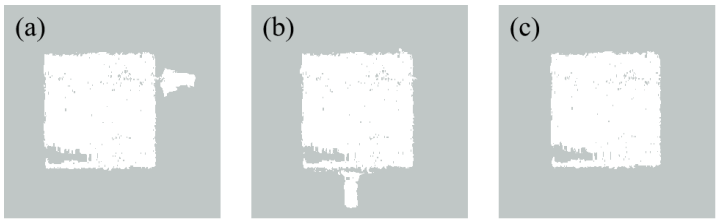

Fig. 3: Comparison of planar prediction results. (a) Region Growing. (b) RANSAC. (c) PCA-RANSAC.

Comparison experiments with the alpha-shapes algorithm [8] are conducted to verify the effectiveness of the proposed algorithm. Despite potential influences from equipment or environmental factors, the chip plane point cloud may not be complete. As depicted in Fig. 4. and summarized in Tab. 1, both algorithms demonstrate the capability to extract the effective boundary, with the algorithm presented in this paper exhibiting superior speed. The boundary points are segmented into multiple segments based on clustering, as shown in Fig. 5.

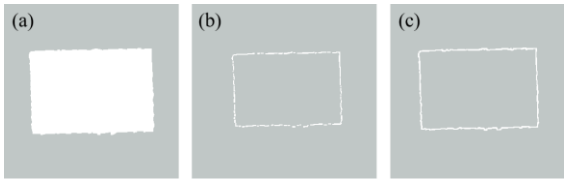

Fig. 4: Boundary extraction comparison. (a) Plane point cloud to be processed. (b)Result by alpha shapes. (c) Result by the proposed method.

Methods	*Number of Points in Point Cloud*	*Number of Boundary Points*	*Cost Time/ms*
Alpha shapes	50884	654	489.735
Our method	50884	935	53.261

Tab. 1: Comparison of contour extraction data.

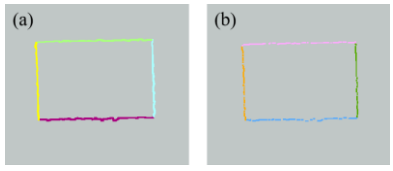

Fig. 5: Boundary point segmentation result. (a) Cluster segmentation results after boundary extraction of the proposed method. (b) Cluster segmentation results after alpha shapes boundary extraction.

The geometry is shown in Fig. 6 and the vertex data is shown in Tab. 2. In order to verify the versatility of the proposed algorithm, a plurality of objects is used to extract the geometry of multiple faces, and the results are shown in Fig.7.

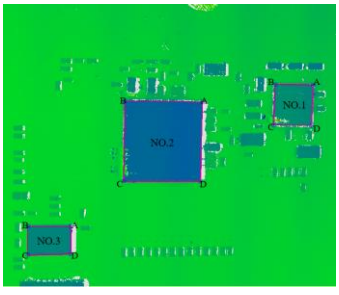

Fig. 6: Chip geometry.

Data	*Point A/mm*	*Point B/mm*	*Point C/mm*	*Point D/mm*
NO.1	(28.254,27.531,1.275)	(31.097,27.468,1.189)	(31.067,24.514,1.187)	(28.221,24.586,1.242)
NO.2	(36.442,25.998,1.550)	(41.974,25.865,1.512)	(41.873,20.150,1.492)	(36.350,20.268,1.525)
NO.3	(48.510,14.689,1.281)	(45.482,14.780,1.284)	(45.526,16.789,1.285)	(48.543,16.740,1.281)

Tab. 2: Geometry vertex measurement data.

This paper introduces a PGE-RANSAC method designed to efficiently and robustly extract point cloud geometry. Experimental results demonstrate that the proposed method effectively extracts geometric features from point clouds, indicating promising prospects for applications in industrial measurement.

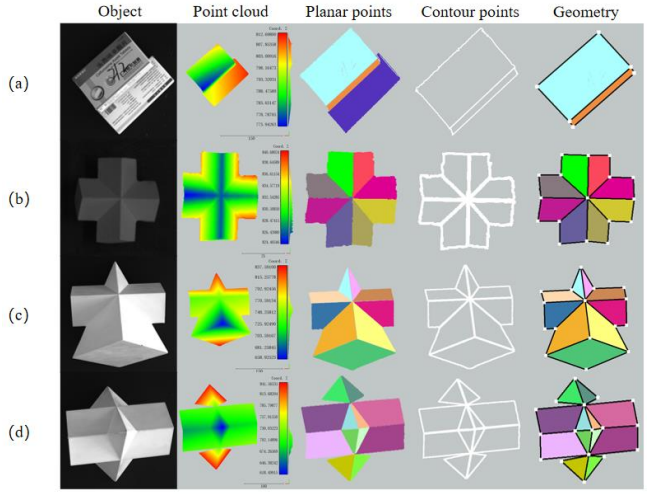

Fig. 7: Diagram of the experimental steps of different objects by the method in this paper. (a-d) are different objects.

References:

[1] Deng, X.; Qiu, S.; Jin, W.; Xue, J. Three-Dimensional Reconstruction Method for Bionic Compound-Eye System Based on MVSNet Network, Electronics, 11, 2022, 1790. https://doi.org/10.3390/electronics11111790

[2] Qiu, S.; Anwar, S.; Barnes, N. Damage Detection Based on 3D Point Cloud Data Processing from Laser Scanning of Conveyor Belt Surface, IEEE Transactions on Multimedia, 24, 2022, 1943-1955. https://doi.org/10.1109/TMM.2021.3074240

[3] Pham, T. T.; Eich, M.; Reid, L.; Wyeth, G. Geometrically consistent plane extraction for dense indoor 3D maps segmentation, 2016 IEEE/RSJ International Conference on Intelligent Robots and Systems (IROS), Daejeon, Korea (South), 9-14 October 2016. https://doi.org/10.1109/IROS.2016.7759618

[4] Nan, L. L.; Wonka, P. PolyFit: Polygonal Surface Reconstruction from Point Clouds. 2017 IEEE International Conference on Computer Vision (ICCV), Venice, Italy, 22-29 October 2017. https://doi.org/10.1109/ICCV.2017.258

[5] Hackel, T.; Wegner, J. D.; Schindler, K. Joint classification and contour extraction of large 3D point clouds, ISPRS Journal of Photogrammetry and Remote Sensing, 130, 2017, 231-245. https://doi.org/10.1016/j.isprsjprs.2017.05.012

[6] Magri, L.; Leveni, F.; Boracchi, G. MultiLink: Multi-class Structure Recovery via Agglomerative Clustering and Model Selection. 2021 IEEE/CVF Conference on Computer Vision and Pattern Recognition (CVPR), Nashville, USA, 20-25 June 2021. https://doi.org/10.1109/CVPR46437.2021.00189

[7] Vo, A-H.; Linh, T-H.; Laefer, D.; Bertolotto, M. Octree-based region growing for point cloud segmentation. ISPRS Journal of Photogrammetry and Remote Sensing, 104, 2015, 88-100. https://doi.org/10.1016/j.isprsjprs.2015.01.011

[8] Edelsbrunner, H.; Mücke, E. Three-dimensional alpha shapes. 3D Research 1994, 2, 1-13. https://doi.org/10.1145/174462.156635